

Variable-stiffness Sheets Obtained using Fabric Jamming and their Applications in Force Displays

Takashi Mitsuda

To cite this article: Takashi Mitsuda (2017): Variable-stiffness Sheets Obtained using Fabric Jamming and their Applications in Force Displays, Proceedings of the IEEE World Haptics Conference (WHC), 364-369. DOI: 10.1109/WHC.2017.7989929

This is an Accepted Manuscript of an article published by IEEE on 27/07/2017, available online:

<http://ieeexplore.ieee.org/document/7989929/>

Variable-stiffness Sheets Obtained using Fabric Jamming and their Applications in Force Displays

Takashi Mitsuda, *Ritsumeikan University*

Abstract—The stiffness of a bag containing particles can be increased by evacuating the air inside it. This stiffness-control technology, referred to as granular jamming, has been used in force displays. In such displays, the operator feels a reaction-force sensation when deforming the bag with a hand motion. The particle-containing bag can be deformed into any shape; however, the bag cannot be converted into a thin plate. This study proposes a sheet-like mechanism that, rather than particles, contains piled-stretch fabrics inside a thin rubber bag. The sheet becomes rigid after evacuating the air from the bag, with stiffness proportional to the vacuum pressure inside the bag as observed in the granular-jamming method. The sheet thickness, which is determined using the number of piled-fabric layers, is approximately in the range of 1–5 mm. The softness and stretchability of the sheet allows it to form a spherical shape and maintain that shape after vacuuming the inner air. This study demonstrates the fundamental properties of a variable-stiffness sheet and its applications in force displays.

I. INTRODUCTION

Most force displays available are robotic arms whose joints are actuated via motors. Other types of force displays, wherein a passive-resistance force is exerted using brakes instead of motors, have also been studied [1, 2]. Passive force displays are safer than conventional displays because excessive force is not exerted, which can otherwise potentially harm the operator. Instead of using conventional brakes, a granular-jamming technology is used in passive force displays, which allows for the variable-stiffness control of a particle-containing bag by evacuating the air inside it. This paper refers to the mechanical element that uses granular jamming as the particle mechanical constraint (PMC). The PMC comprises a soft plastic bag that contains particles such as polystyrene foam beads and coffee beans. Hence, it is soft, lightweight, and suitable for systems that interact with the human body.

Mitsuda et al. [3] developed a wearable force display wherein a cylindrical PMC fixed on an operator's trunk below the arm helps in constraining the hand motion (Fig. 1 (a)). This display allows operators to move their hands freely in any direction with the help of the soft, lightweight mechanism. PMCs have also been used in other types of force displays. Glove-type force displays help in constraining the finger motion using PMCs fixed on or under the glove (Fig. 1 (b)) [4–6]. In tabletop-type force displays, the hand or finger motion is constrained using PMCs that help connect the body of the operator to the ground (Figs. 1 (c) and (d)) [7–10]. In handheld-type force displays, a force sensation is directly produced via the stiffness of the PMC, which the operator grips with his/her hand (Fig. 1 (e)) [11]. PMCs have been also

used for controlling the stiffness of soft robotic arms [12–16] or deformable robots [17–19].

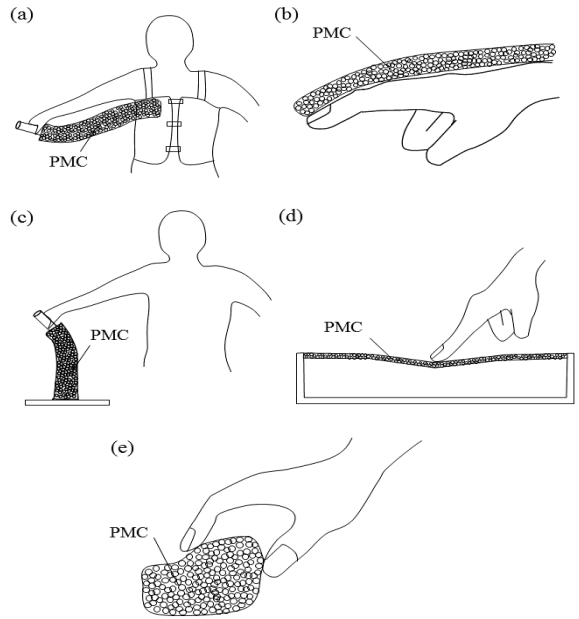


Figure 1. Force displays developed using granular-jamming technology; (a) wearable force display, (b) glove-type display, (c) and (d) tabletop-type displays, and (e) handheld-type display

PMCs can be deformed into various shapes, which is one of the reasons for their wide application. However, it is difficult to convert PMCs into a thin plate because the particles inside the PMC are not always evenly distributed without gaps. Because the particles freely move with the effect of gravity, large gaps between the particles often appear inside the bag when it is bent or is placed vertically (Fig. 2). The spatial inhomogeneity in the particle distribution can be prevented by equally dividing the particles using a gas-permeable sheet [20]. However, such a separation complicates the simple structure and otherwise easy production process of PMCs.

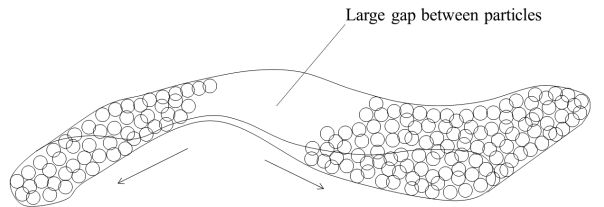


Figure 2. Large gaps between particles when thin PMC is bent or is placed vertically

*Research supported by MEXT-Supported Program for the Strategic Research Foundation.

Takashi Mitsuda is a member of the College of Information Science and Engineering, Ritsumeikan University, Kusatsu, Shiga, 525-8577 Japan (phone/fax: +71-77-561-5068; e-mail: mitsuda@is.ritsumei.ac.jp).

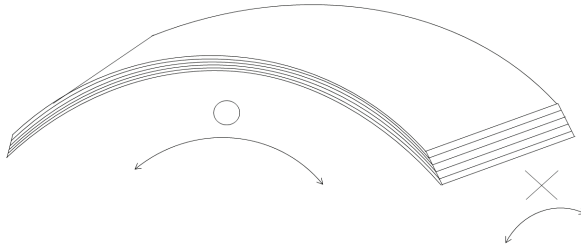


Figure 3. Deformation of variable-stiffness sheet containing piled-plastic films

To solve this limitation of PMCs, this study proposes a variable-stiffness sheet that contains piled-stretch fabrics instead of particles. In this study, the sheet is referred to as the fabric-jamming sheet (FJS). As in PMCs, the stiffness of the FJS is proportional to the inside vacuum pressure. The thickness is determined using the number of piled fabrics, and is approximately 1 mm when 16 mesh sheets are piled and contained in a rubber bag.

In a similar technology, the variable-stiffness sheets containing piled-plastic films have been used in haptic displays [21, 22]. Recently, these sheets have been employed in a membrane of soft robotic arms, which is referred to as layer jamming [23, 24]. The differences between the FJS and the layer-jamming sheet lie in their flexibility and stretchability. The piled-plastic films used in the layer-jamming sheet can bend only in one direction, and not in two directions simultaneously (Fig. 3). In contrast, the piled fabrics used in the FJS can fit on a spherical surface owing to their stretchability. The piled-plastic films can be made to fit on a spherical surface by employing a woven structure with strip-shaped films [25]. The variable-stiffness plates comprising plastic films capable of fitting on a spherical surface have been suggested [26]. However, the deformability of these mechanisms is limited by the size and nonstretchability of the films.

In this paper, the structure and fundamental mechanical properties of the FJS are presented. A glove-type force display and a tabletop-type force display developed using the FJS are presented.

II. STRUCTURE

Fig. 4 shows the structure of the FJS containing the piled-stretch fabrics. The stretch fabrics made of nonelastic fibers (such as polyester) are piled, and subsequently, covered with a rubber bag. The air inside the bag is evacuated through a fixed air tube. As shown in Fig. 5 (a), the fabrics are elongated by changing the shape of the meshes rather than elongating the fibers of the fabric. The entire sheet comprising piled fabrics and a rubber bag is as elastic as a rubber sheet. When the air inside the bag is evacuated, the atmospheric pressure helps in bonding the piled fabrics tightly. They become hard because the deformation of the meshes is disturbed by the friction due to adherence. The sheet can be fixed in any shape by evacuating the inner air, and can be released by inflating the sheet. The material of the

fabric should be nonelastic. When the material is elastic, the sheet becomes softer. However, the stiffness of the FJS using elastic fibers is lower than that of the FJS using non-elastic fibers. In this study, the material used for the fabric is polyester. The FJS has the following advantageous over PMC:

Thinness: The thickness of the FJS is determined using the number of fabric layers. The thickness of a fabric layer used in this study (Fig. 5 (b)) is approximately 0.04 mm. The thicknesses of the FJS, including the rubber bags (0.34 mm), are 0.7, 0.9, 1.7, 2.3, and 4.0 mm for the FJS containing 8, 16, 32, 48, and 96 piled-fabric layers, respectively. As mentioned previously, it is difficult to obtain a thin PMC without having gaps between the particles (Fig. 2). The thinness of the FJS can help extend the range of application.

Elasticity: The developed FJS is elastic because the fabric layers and rubber bag are stretchable. The material of the bag used in the PMC should be nonelastic (e.g., polyvinyl chloride). If an elastic material, such as rubber, is used in the PMC, the elongation stiffness decreases drastically. In contrast, the developed sheet has higher elongation stiffness than the PMCs made of an elastic bag because the piled fabrics adhere together and resist elongation. The maximum elongation ratio of the FJSs developed in this study is approximately 200% in the horizontal and vertical directions. The elasticity allows for variable deformation without inducing large wrinkles (Fig. 6). When a PMC made of a nonelastic bag is bent or compressed, wrinkles appear, which can sometimes decrease the stiffness of the PMC.

Responsiveness: The response time of the stiffness control for both PMCs and FJS is determined using the air capacity inside the bag as well as the vacuuming speed of the vacuum pump. The air capacity of the FJS is lower than that of PMCs because the FJS is thin.

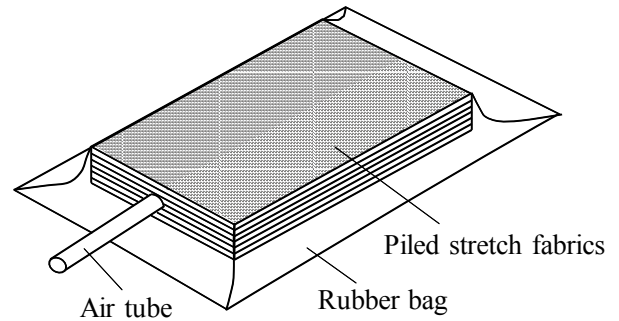


Figure 4. Structure of fabric-jamming sheet

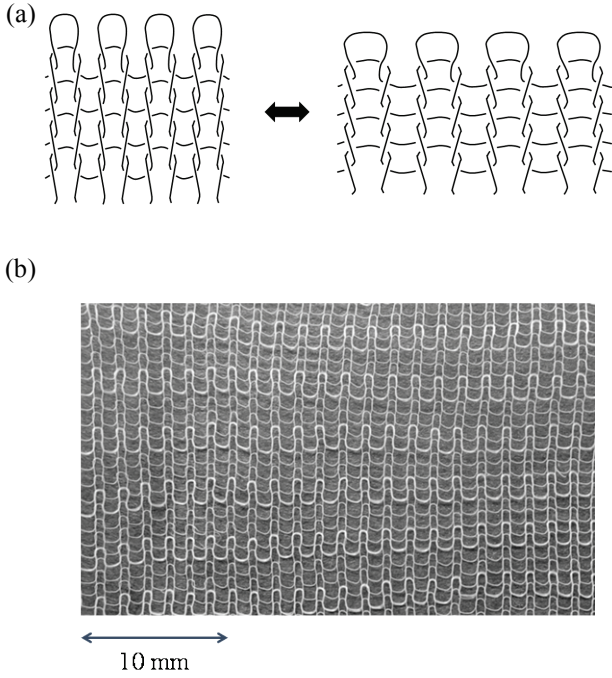


Figure 5. (a) Elongation of a stretch fabric, and (b) image of a stretch fabric



Figure 6. Deformation of fabric-jamming sheet. This image shows a fabric-jamming sheet obtained by evacuating the inner air after deforming with hand.

III. MECHANICAL PROPERTIES

A. Anisotropic elongation stiffness of piled fabrics

The elongation stiffness of an FJS, comprising stretch fabrics (width of 160 mm and depth of 160 mm) piled in the same direction, was analyzed by measuring the reaction force when the central part of the FJS (width of 20 mm and distance of 30 mm) was elongated at a speed of 50 mm/min, as shown in Fig. 7. The inside vacuum pressure was -92 kPa.

The continuous and dotted lines in Fig. 8 indicate the stiffness of the FJS when elongated in the horizontal (see Fig. 5) and orthogonal (vertical) directions, respectively. Anisotropic behavior was clearly observed in the elongation stiffness—the stiffness in the horizontal direction was twice that in the vertical direction. The broken lines in Fig. 8 indicate the elongation stiffness of the FJS, wherein the stretch fabrics were piled alternately in the two orthogonal directions, as shown in Fig. 9 (b). The stiffness was largely equal to the

horizontal stiffness of the FJS wherein the fabrics were piled in the same direction. These results demonstrate that alternately arranging the pile of fabrics is advantageous as the stiffnesses are largely equal in both the directions.

In the following analyses, the FJS, wherein the stretch-fabric layers were piled alternately in the two orthogonal directions, were measured using the process shown in Fig. 8.

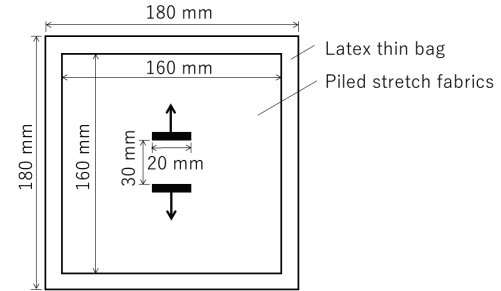


Figure 7. Measurement of the elongation stiffness

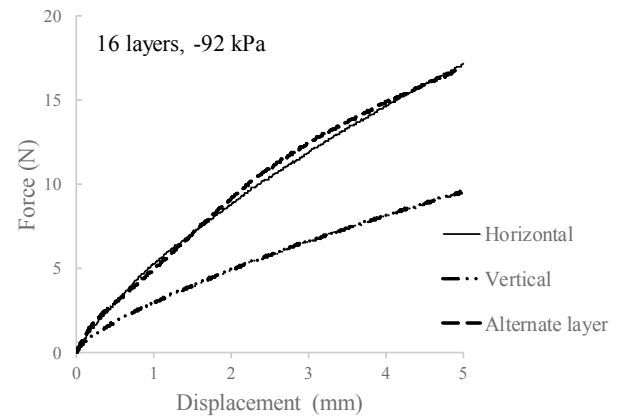


Figure 8. Anisotropic behavior of elongation stiffness

(a) Pile in the same direction (b) Pile alternately in the two orthogonal directions

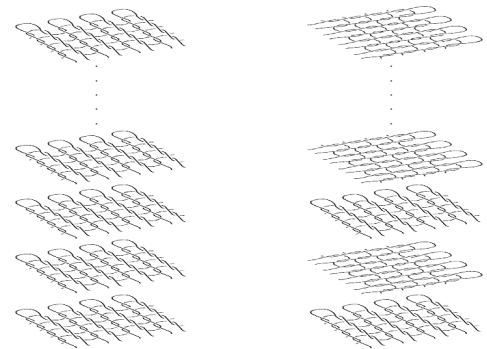


Figure 9. Stretch fabrics piled either in the same direction or alternately in the two orthogonal directions

B. Number of stretch-fabric layers

Fig. 10 shows the elongation stiffnesses of the FJSs obtained using different number of stretch-fabric layers. The elongation stiffness of the FJSs can be increased by increasing the number of fabric layers. The increase in stiffness was largely proportional to the number of fabric layers, but not when the number of layers was 48 and 96, which requires further analysis.

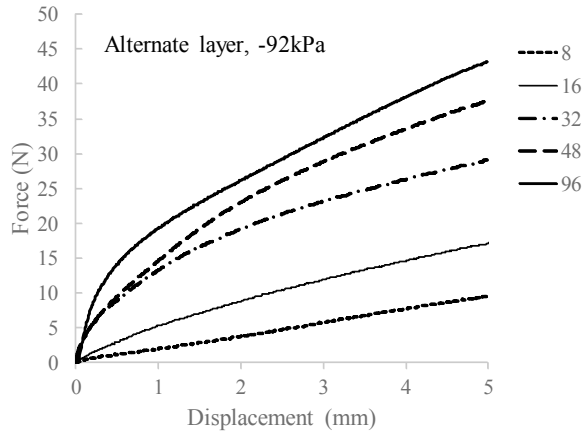


Figure 10. Elongation stiffnesses of sheets obtained using different number of fabric layers

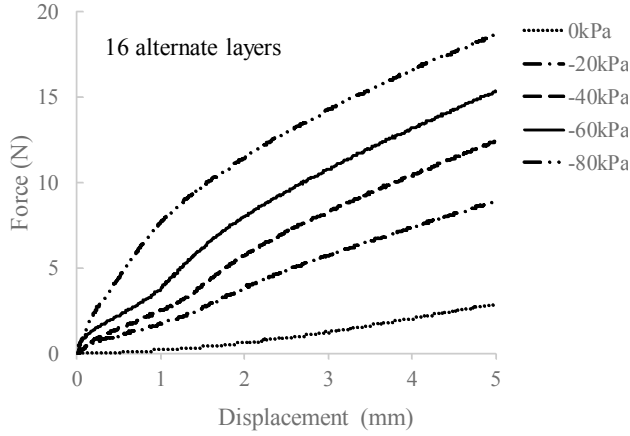


Figure 11. Elongation stiffnesses of sheets with different inner vacuum pressures

C. Inner vacuum pressure

Fig. 11 shows the elongation stiffnesses of the FJSs obtained using 16 fabric layers at different inner pressures. The figure shows that the stiffness increases with the increase in the interior vacuum pressure, which is in accordance with the PMCs.

IV. FORCE DISPLAYS

A. Tabletop-type force display

A tabletop-type force display was developed using an FJS with 32 piled fabrics, as shown in Fig. 1 (d). The FJS was fixed on a cylinder with a diameter of 88 mm. The reaction force obtained by pushing the center of the FJS with a 15-mm-diameter rod was measured, as shown in Fig. 12. Fig.

13 shows the results, which indicate that the reaction force can be controlled via the vacuum pressure inside the FJS. When an FJS with 96 piled fabrics (as opposed to 32 piled fabrics) was used in the force display, the reaction forces at a displacement of 10 mm were 26.8 and 1.5 N for inner pressures of -80 kPa and atmospheric pressure, respectively.

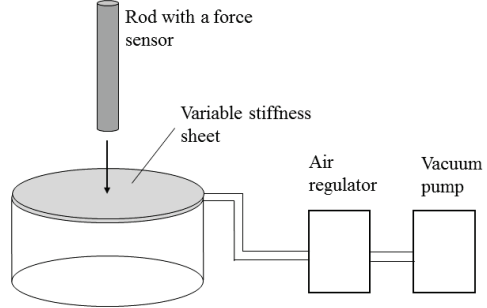


Figure 12. Tabletop-type force display and reaction-force measurement

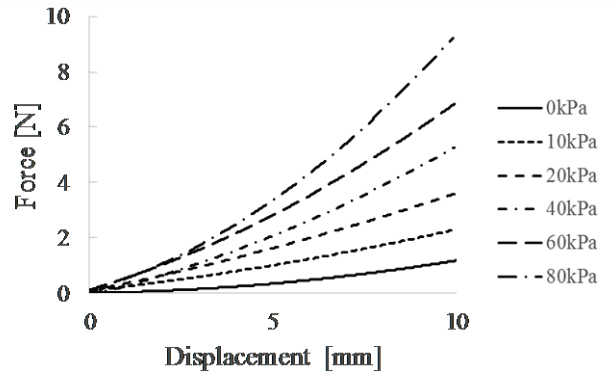


Figure 13. Reaction forces of tabletop-type force display using fabric-jamming sheet

B. Glove-type force display

A glove-type force display was developed using FJSs with 32 piled fabrics. Fig. 14 shows the schematic structure of the force display. The piled fabrics (each with a width of 15 mm and a length of 20 mm), which were serially connected using plastic plates, were sealed in an inner latex glove and were connected with an air tube. The inner glove was fixed with the outer latex glove where the piled fabrics were located on the digital joints. The stiffness and disturbed finger motion increased by evacuating the air inside the inner glove. Fig. 15 shows the reaction force of the index finger at different vacuum pressures when bending the finger, which is measured as a pressure on the finger pad using a pressure sensor (AMI3037-SB, AMI Techno co., ltd., JAPAN). A circular sensor probe (diameter 2 cm) was fixed on the finger pad. The measurements were repeated three times for each vacuum pressure. Fig. 16 shows the results. As shown in the figure, the reaction force is approximately proportional to the inner vacuum pressure. The reaction force (i.e., pressure on

the finger pad) at atmospheric pressure is due to the elasticity of the latex glove and FJSs, which need to be improved. In this force display, a reaction force is exerted on all areas of the fingers because the FJS is directly fixed on the finger. Thus, the pressure was measured in this experiment and not the force. The reaction force on the sensor probe is approximately 1.6 N when the pressure is 5 kPa.

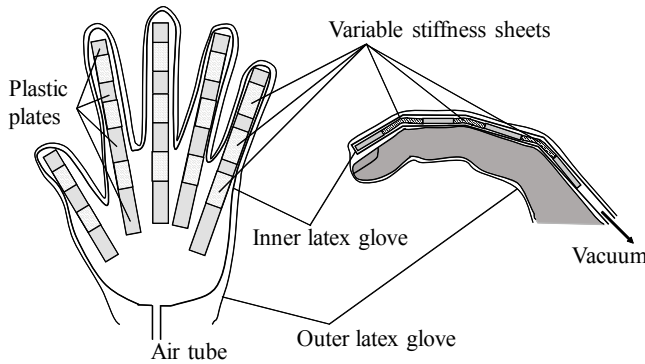


Figure 14. Schematic of glove-type force display using fabric-jamming sheets

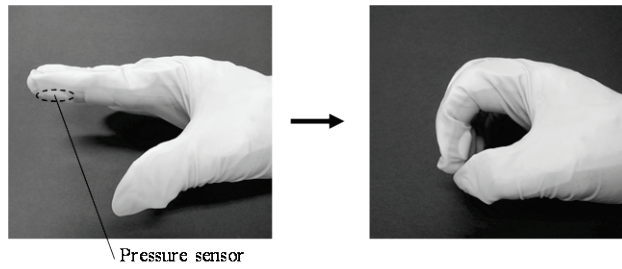


Figure 15. Grasping motion of glove-type force display for measuring the reaction force

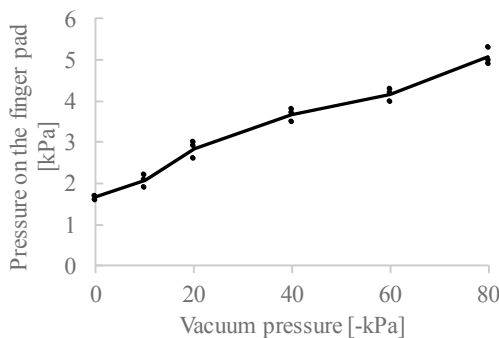


Figure 16. Reaction forces of the glove-type force display using fabric-jamming sheets. The solid lines connect the means of reaction forces at each inside vacuum pressure

V. CONCLUSION

The novel FJSs are applicable not only to force displays but also to medical casts, supports, soft robot mechanical elements, fixing devices, etc. In future, the FJS can be improved by incorporating the following factors.

1. Optimal materials and structures should be explored for

the piled-mesh sheet to increase the maximum stiffness and decrease thickness.

2. A structure should be developed that can maintain the thinness. The thickness of the variable sheet developed in this study was greater when the inner air pressure was at atmospheric levels than when it was at vacuum levels because the piled-stretch fabrics are fluffy. This larger thickness leads to increased air capacity and reduced response speed.

REFERENCES

- [1] J. Furusho and R. Sakaguchi, "New actuators using ER fluid and their applications to force display devices in virtual reality and medical treatments," *International Journal of Modern Physics B*, vol. 13, no. 14-16, pp. 2151–2159, Jun 1999.
- [2] D. Ryu, K. Moon, S. C. Kang, M. Kim, and J. B. Song, "Development of wearable haptic system for tangible studio to experience a virtual heritage alive," in *Conf. Rec. 2006 IEEE/RSJ International Conference on Intelligent Robots and Systems*, pp. 466–471.
- [3] T. Mitsuda, S. Kuge, M. Wakabayashi, and S. Kawamura, "Wearable force display using a particle mechanical constraint," *Presence-Teleoperators and Virtual Environments*, vol. 11, no. 6, pp. 569–577, Dec 2002.
- [4] T. Mitsuda and S. Kawamura, "Development of a haptic display with Particle Mechanical Constraints," in *Conf. Rec. 2002 JSME Conference on Robotics and Mechatronics*, 1P1-F10. (in Japanese)
- [5] T. M. Simon, R. T. Smith, and B. H. Thomas, "Wearable jamming mitten for virtual environment haptics," in *Proc. 2014 ACM Int'l Symp. Wearable Computers*, pp. 67–70, 2014.
- [6] I. Zubrycki and G. Granosik, "Novel haptic glove-based interface using jamming principle," *2015 10th International Workshop on Robot Motion and Control*, pp. 46–51.
- [7] T. Mitsuda, S. Kuge, M. Wakabayashi, and S. Kawamura, "Haptic displays implemented by controllable passive elements," in *Conf. Rec. 2002 IEEE International Conference on Robotics and Automation*, pp. 4223–4228.
- [8] A. M. Genecov, A. A. Stanley, and A. M. Okamura, "Perception of a haptic jamming display: just noticeable differences in stiffness and geometry," *IEEE Haptics Symposium*, pp. 333–338, 2014.
- [9] M. Li et al., "Multi-fingered haptic palpation utilizing granular jamming stiffness feedback actuators," *Smart Materials and Structures*, vol. 23, no. 9, Art. no. 095007, 2014.
- [10] A. A. Stanley and A. M. Okamura, "Controllable surface haptics via particle jamming and pneumatics," *IEEE Trans. on Haptics*, vol. 8, no. 1, pp. 20–30, 2015.
- [11] S. Follmer, D. Leithinger, A. Olwal, N. Cheng, and H. Ishii, "Jamming user interfaces: programmable particle stiffness and sensing for malleable and shape-changing devices," *UIST'12: Proceedings of the 25th Annual ACM Symposium on User Interface Software and Technology*, pp. 519–528, 2012.
- [12] N. G. Cheng et al., "Design and analysis of a robust, low-cost, highly articulated manipulator enabled by jamming of granular media," in *Conf. Rec. 2012 IEEE International Conference on Robotics and Automation*, St Paul, MN, pp. 4328–4333.
- [13] A. Jiang et al., "Design of a variable stiffness flexible manipulator with composite granular jamming and membrane coupling," in *Conf. Rec. 2012 IEEE/RSJ International Conference on Intelligent Robots and Systems*, pp. 2922–2927.
- [14] T. Yanagida, K. Adachi, and T. Nakamura, "Development of endoscopic device to veer out a latex tube with jamming by granular materials," in *Conf. Rec. 2013 IEEE international conference on robotics and biomimetics*, pp. 1474–1479.
- [15] M. Cianchetti et al., "Soft robotics technologies to address shortcomings in today's minimally invasive surgery: the STIFF-FLOP approach," *Soft Robotics*, vol. 1, no. 2, pp. 122–131, Jun 2014.
- [16] T. Ranzani, M. Cianchetti, G. Gerboni, I. De Falco, and A. Menciassi, "A soft modular manipulator for minimally invasive surgery: design

- and characterization of a single module,” *IEEE Trans. on Robotics*, vol. 32, no. 1, pp. 187–200, Feb 2016.
- [17] A. Mazzone, C. Spagno, and A. Kunz, “The HoverMesh: a deformable structure based on vacuum cells: new advances in the research of tangible user interfaces,” in *Proc. of the 2004 ACM SIGCHI International Conference on Advances in computer entertainment technology*, pp. 187–193.
 - [18] E. Steltz, A. Mozeika, N. Rodenberg, E. Brown, and H. M. Jaeger, “JSEL: Jamming Skin Enabled Locomotion,” in *Conf. Rec. 2009 IEEE-RSJ International Conference on Intelligent Robots and Systems*, pp. 5672–5677.
 - [19] E. Steltz, A. Mozeika, J. Rembisz, N. Corson, and H. M. Jaeger, “Jamming as an Enabling Technology for Soft Robotics,” in *Conf. Rec. 2010 Conference on Electroactive Polymer Actuators and Devices*, San Diego, CA, vol. 7642.
 - [20] T. Mitsuda, S. Kuge, M. Wakabayashi, and S. Kawamura, “Wearable haptic display by the use of a particle mechanical constraint,” *10th Symposium on Haptic Interfaces for Virtual Environment and Teleoperator Systems*, pp. 153–158, 2002.
 - [21] S. Kawamura et al., “Development of passive elements with variable mechanical impedance for wearable robots,” in *Conf. Rec. 2002 IEEE International Conference on Robotics and Automation*, pp. 248–253.
 - [22] S. Kawamura, K. Kanaoka, Y. Nakayama, J. Jeon, and D. Fujimoto, “Improvement of passive elements for wearable haptic displays,” in *Conf. Rec. 2003 20th IEEE International Conference on Robotics and Automation*, Taipei, Taiwan, pp. 816–821.
 - [23] Y. J. Kim, S. B. Cheng, S. Kim, and K. Iagnemma, “A novel layer jamming mechanism with tunable stiffness capability for minimally invasive surgery, *IEEE Trans. on Robotics*, vol. 29, no. 4, pp. 1031–1042, Aug 2013.
 - [24] J. L. C. Santiago, I. D. Walker, and I. S. Godage, “Continuum robots for space applications based on layer-jamming scales with stiffening capability,” in *Conf. Rec. 2015 IEEE Aerospace Conference*, pp. 1-13.
 - [25] J. Ou et al., “JamSheets: thin interfaces with tunable stiffness enabled by layer jamming,” in *Proc. 8th Int'l Conf. Tangible, Embedded and Embodied Interaction*, pp. 65–76, 2014.
 - [26] T. Mitsuda and N. Matsuo, “Shape stabilizer using an articulation-type passive element,” *JFPS Int. Symp. on Fluid Power*, pp. 723–727, 2005.